Journal of Mechanics in Medicine and Biology
Vol. 12, No. 2 (2012) 1240004 (13 pages)

DOI: 10.1142/S0219519412400040

INVESTIGATING DIFFERENT TARGETS IN DEEP BRAIN STIMULATION ON PARKINSON'S DISEASE USING A MEAN-FIELD MODEL OF THE BASAL GANGLIA-THALAMOCORTICAL SYSTEM

ALIREZA NAHVI* and FARIBA BAHRAMI
CIPCE, School of Electrical and Computer Engineering
College of Engineering, University of Tehran
P.O. Box 1391843953, Tehran, Iran
**a.nahvi@ece.ut.ac.ir*

SAMIRA HEMMATI
School of Industrial Engineering
College of Engineering, University of Tehran
P.O. Box 1391843953, Tehran, Iran

Received 2 June 2011
Revised 16 October 2011
Accepted 19 November 2011

In this paper, we investigated effects of deep brain stimulation (DBS) on Parkinson's disease (PD) when different target sites in the basal ganglia are stimulated. The targets which are investigated are subthalamic nucleus (STN), globus pallidus interna (GPi), and globus pallidus externa (GPe). For this purpose we used a computational model of the basal ganglia-thalamocortical system (BGTCS) with parameters calculated for mean field. This model is able to reproduce both the normal and Parkinsonian activities of basal ganglia, thalamus and cortex in a unified structure. In the present study, we used a mean-field model of the BGTCS, allowing a more complete framework to simulate DBS and to interpret its effects in the BGTCS. Our results suggest that DBS in the STN and GPe could restore the thalamus relay activity, while DBS in the GPi could inhibit it. Our results are compatible with the experimental and the clinical outcomes about the effects of DBS of different targets.

Keywords: Mean field model; basal ganglia-thalamocortical system; Parkinson's disease; deep brain stimulation.

1. Introduction

The basal ganglia are related to various motor and cognitive disorders, such as Huntington's disease, Parkinson's disease (PD), and schizophrenia.[1–3] James Parkinson for the first time described Parkinson's disease (PD) in 1817.[4] PD is a syndrome with symptoms including slowness of movement (bradykinesia), difficulty in initiating movements (akinesia), rigidity, and rest tremor. PD occurs due to decreased

dopamine release in the substantia nigra pars compacta (SNc). Parkinsonism leads to different changes in discharge rates of the basal ganglia-thalamocortical system (BGTCS), often including increase in Mean Firing Rates (MFR) of the subthalamic nucleus (STN) and the globus pallidus pars interna (GPi) which is the output nucleus of the basal ganglia to the thalamus. PD also decreases MFR of the globus pallidus pars externa (GPe) and thalamic relay nucleus.[5,6] Contribution of basal ganglia to akinesia, bradykinesia, and rigidity is concluded by the fact that STN or globus pallidus lesions or Deep Brain stimulation can improve these symptoms.[7–9]

Deep brain stimulation (DBS), in the basal ganglia is a proper method to help Parkinson patients whose response to medication is not in an appropriate manner relative to their status. Despite the increasing use of spread deep brain stimulation, an important point is that the mechanism of this method is not known precisely and clearly.[10] Therefore, modeling is considered as a non-invasive method to study the behavior of neurons and their response to electrical stimulation. A few computational models in the field of brain stimulation are available. These models describe limited and incomplete structure of the BG (see Refs. 11 and 12 for example). Some of these models are mainly used to study effects of stimulation of nuclei such as STN, GPe and GPi in PD. Existing models use the high number of cells (neuronal population model) to describe the electrophysiological behavior of nuclei.

For example, Rubin and Terman presented a model of basal ganglia, including STN, GPi, GPe, and thalamus.[11] Each nucleus in this model was expressed by a Hodgkin–Huxley model with parameters adjusted for the population neurons. In RTM (Rubin and Terman Model), the striatum and the STN are considered the input ports of the BGS, while the GPi and the SNr are the output ports of the BGS projecting to the thalamus and brainstem targets. In this model, the thalamus is a simple relay station whose physiological role is to faithfully respond to the inputs arriving from the sensorimotor cortex (SMC). Thalamic cells receive also inhibitory inputs from the GPi cells. In the physiological state of the RTM the GPi activity is tonic and uncorrelated among subpopulations of the GPi cells and do not disrupt the thalamic relay activity. In the PD state of the RTM the GPi activity is phasic and correlated among subpopulations of the GPi cells and disrupt the thalamic relay activity. They showed how the high frequency STN-DBS eliminates pathological thalamic activity.

Another BG model is presented by Modolo and colleagues, and includes only STN and GPe.[12] Each neuron is modeled using Izhikevich model with modified parameters estimated based on the neurophysiologic properties of STN. In this model, the STN-GPe complex dynamics are expressed by two partial differential equations. They investigated the argument suggesting the effects of DBS in PD could be a combination of functional decoupling and resonant properties of STN neuron membranes. One limitation of this model is that it expresses the interactions of only two nuclei of the BG, and interactions of other nuclear such as GPi and the thalamus have not been considered.

In this study, we used a BGTCS model Ref. 13 to investigate the effects of deep-brain stimulation of different targets in the BG (stimulating STN and GP). This model includes complete circuitry of the basal ganglia (all nuclei and their interactions) and considers all pathways and therefore is more reliable than other existing models. In the BGTCS model, firing rate characteristics of all BG nuclei are reproduced. To avoid the complexity of the model we have used a mean field model (similar to Ref. 13). The purpose of this paper is to compare the effect of different DBS targets. To this end, we illustrate how high-frequency stimulation of BG nuclei may facilitate signal transmission by the thalamus in Parkinsonian patients.

The main features of the BGTCS model are presented in Sec. 2. Section 3 details the simulation results. Simulation results are then compared with experimental and clinical evidences in Sec. 4. Finally, the concluding remarks are provided in Sec. 5.

2. Methods

2.1. *Software tools*

The BGTCS has been implemented with MATLAB 7.8, on a PC platform (Intel Core 2 Duo CPU T9300 @ 2.5 GHz, 4 GB of RAM).

2.2. *Features of the model*

Here, we use a mean field instead of the neuronal population model. Dynamics of each neuron is described using the model introduced in Ref. 13. In this model, neuronal properties are spatially averaged. The dynamics are then governed by a set of equations relating the average firing rates of neuron populations to changes in cell-body potential, which are in turn triggered by average rates of incoming pulses.

Basic sets of equations of the BGTCS are presented here. See Ref. 13 for more details on parameters and equations used.

The mean firing rate Q_a is related to the cell-body potential V_a by the below equation

$$Q_a(V_a) = S_a(V_a) = Q_a^{\max}/(1 + \exp[-(V_a - \theta_a)/\sigma'\,]). \tag{1}$$

Here features of this equation are presented: $Q_a^{\max}$ is the maximum attainable firing rate, α is the subscript of populations, θ_a is the mean threshold potential, and σ' is $\sqrt{3}/\pi$ times the standard deviation of the Gaussian distribution of firing thresholds.

The cell-body potential V_a is related to the change in the mean cell-body potential υ_{ab} by the below equations

$$D_{a\beta}(t)V_a(t) = \sum_b \upsilon_{ab}\Phi_b(t - \tau_{ab}), \tag{2}$$

$$D_{a\beta}(t) = (1/\alpha\beta)\partial^2/\partial t^2 + (1/\alpha + 1/\beta)\partial/\partial t + 1. \tag{3}$$

Here features of these equations are presented: Φ_b is the incoming pulse rate, τ_{ab} is the axonal time delay for signals traveling from type b to type a neurons, and α and β are the decay and raise rates of the cell-body potential.

The mean firing rate Q_a is related to the incoming pulse rate Φ_a by below equation.

$$(1/\alpha\beta)[\partial^2/\partial t^2 + 2\gamma_a \partial/\partial t + \gamma_a^2]\Phi_a(t) = Q_a(t). \tag{4}$$

Here features of this equation are presented: γ_a is the damping rate.

Stable steady states of the model equations, obtained assuming a constant input Φ_a and setting the derivatives in previous equations to zero: $\Phi_a^{(0)} = Q_a^{(0)}$, and $S_a^{-1}(\Phi_a^{(0)}) = \sum_b \upsilon_{ab}\Phi_b^{(0)}$; then, we have the below equation

$$\Phi_a^{(0)} = Q_a^{\max} \Bigg/ \left[1 + \exp\left[-\left(\left(\sum_b \upsilon_{ab}\Phi_b^{(0)}\right) - \theta_a\right)\Big/\sigma'\right]\right]. \tag{5}$$

These equations are simplified by imposing the random connectivity approximation; this implies, in particular, that the fixed-point values of the cortical excitatory and inhibitory firing rate fields are equal. Finally the main equation that will be used in this paper is presented here

$$\Phi_a = Q_a^{\max} \Bigg/ \left(1 + \exp\left[-\left(\left(\sum_b \upsilon_{ab}\Phi_b\right) + \upsilon_{a\,\text{stimuli}}\Phi_{\text{stimuli}} - \theta_a\right)\Big/\sigma'\right]\right). \tag{6}$$

Here a is the subscript of nuclei, Φ_a is mean firing rate, $Q_a^{\max}$ is maximum attainable firing rate, υ_{ab} is change in the mean cell-body potential, Φ_b is incoming pulse rate, θ_a is mean threshold potential, and σ' is $\sqrt{3}/\pi$ times the standard deviation of the Gaussian distribution of firing thresholds. The relevant parameters for healthy subjects have been extracted from Ref. 13. These values are presented in appendix.

In Fig. 1 we illustrated the nine nuclei of model: two cortical nuclei including one excitatory (e), and one inhibitory (i), striatal cells projecting to the GPi (d1), striatal cells projecting to GPe (d2), GPi/SNr (p1), GPe (p2), STN (s), thalamic relay nuclei (t), and TRN (r) and input from the brainstem to the thalamus.

We used the model equations from Ref. 13 to obtain stable steady states for MFR of different nuclei of basal ganglia, thalamus and cortex. Since the low-firing-rate steady state for rate of thalamic relay nucleus is stable and yields the most realistic firing rates for all populations, we will consider this steady state to represent the physiological situation.[13] See Ref. 13 for details on equations of the BGTCS and parameter values.

In order to validate our results, we have to compare simulation results with experimental evidences and clinical outcomes. In this way, we will be also able to assess the model by studying the MFR of neurons of different nuclei of basal ganglia after stimulation of each one of STN or GP nuclei.

2.3. *Normal and PD states*

We use following parameters to model the transition between normal and PD states in the model[13]: a combination of a stronger indirect pathway ($\upsilon_{p2d2} = -0.3\,\text{mV}\cdot\text{s}$ for physiological normal state and $\upsilon_{p2d2} = -0.8\,\text{mV}\cdot\text{s}$ for pathological state), and

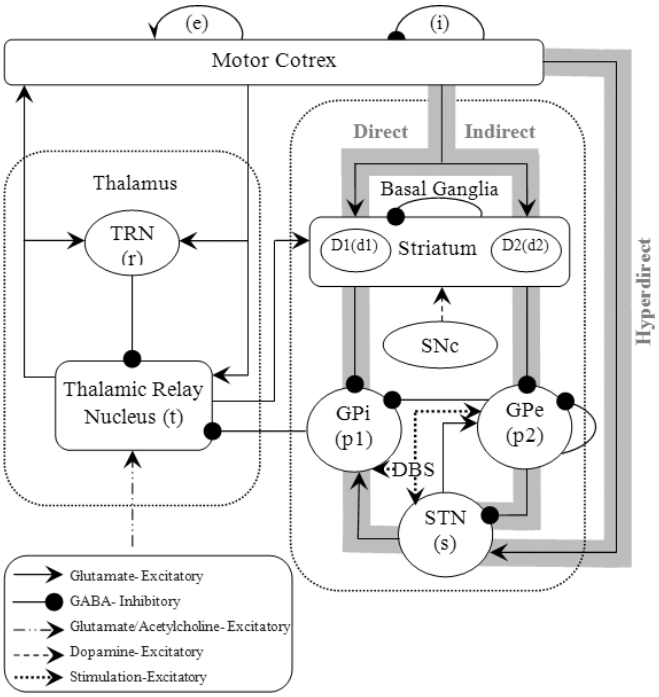

Fig. 1. Structures and connections of the BGTCS.[13] Input from the brainstem reaches the thalamus relay nucleus. Subscripts in parentheses are corresponding to each element. The direct, indirect, and hyperdirect pathways are shown by gray arrows. DBS is alternatively applied in STN, GPe, or GPi in our simulations.

weaker STN firing threshold ($\theta_s = 12\,\text{mV}$ for physiological normal state and $\theta_s = 11.5\,\text{mV}$ for pathological state). The increase in connection strength from striatum to the GPe for the PD state follows the models of PD that propose an "increased response to excitatory input" in the indirect pathway of the basal ganglia due to the decreased activation of D2 receptors in the striatum.[13,14] Lower STN threshold explained the relatively large increase in STN rate observed experimentally.[13,14]

2.4. *Modeling the DBS*

In this model, the DBS was modeled as a positive pulse train that is an input signal into the target nuclei (one at each time). For ensuring an approximately 1:1 ratio between DBS rate and output rate in the target structures, the connection strength was set to 0.08, 0.22 and 0.03 $\text{mV} \cdot \text{s}$ for STN, GPe and GPi stimulation, respectively.

DBS was always tested on the Parkinsonian state of the model.

3. Result

Effects of STN-DBS, GPe-DBS, and GPi-DBS in the model are illustrated in the following subsections. The mean firing rates of STN, GPe, GPi, and thalamic relay nucleus will be discussed.

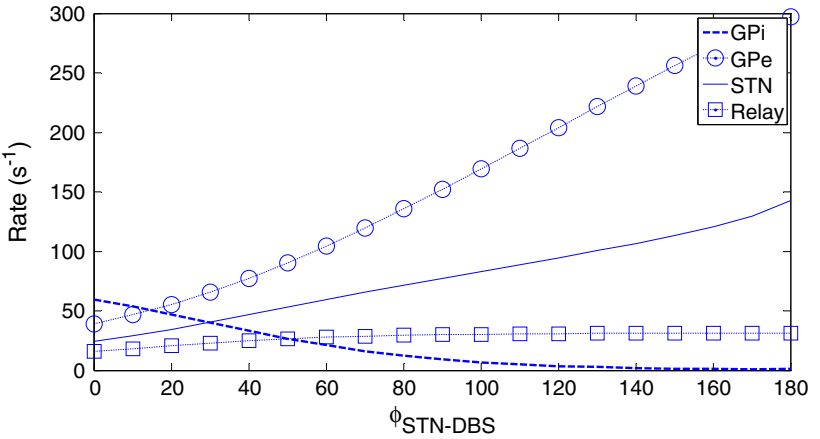

Fig. 2. Mean firing rates of GPi, GPe, STN, and thalamic relay nucleus during STN-DBS. Dashed, GPi; circle-dotted, GPe; solid, STN; square-dotted, thalamic relay nucleus.

3.1. *STN-DBS*

Here DBS was applied to STN. Changes in firing rates due to STN-DBS are shown in Fig. 2.

For DBS up to 120 Hz, the rate of STN increases with DBS. GPe excited by STN, and its rate ascends due to DBS. The resulting contributions to GPi lead it to decrease in its rate. Finally the rate of thalamic relay nucleus increases during DBS.

For DBS above 120 Hz, the rates of STN and GPe still increase with the DBS stimuli. The total inhibition from GPe activity conquest the total excitation from the STN activity and GPi cells were completely inhibited by the inhibitory GPe activity. The rate of thalamic relay nucleus has fixed values during increase in DBS frequency.

3.2. *GPe-DBS*

Here DBS was applied to GPe. Changes in firing rates due to GPe-DBS are shown in Fig. 3.

For DBS up to 40 Hz, the rate of GPe increases with DBS. The rate of STN increases slightly with DBS. The rate of GPi decreases due to DBS same as STN-DBS. And finally the rate of thalamic relay nucleus increases during DBS in like manner to STN-DBS.

For DBS between 40 Hz and 90 Hz, the rate of GPe still increases with DBS. But the rate of STN decreases with DBS. The rate of GPi decreases due to DBS same as STN-DBS. The rate of thalamic relay nucleus increases during DBS in like manner to STN-DBS.

For DBS between 90 Hz and 120 Hz, the rate of GPe still increases with DBS. The rates of STN and GPi still decrease with DBS. The rate of thalamic relay nucleus has fixed values during increase in DBS frequency.

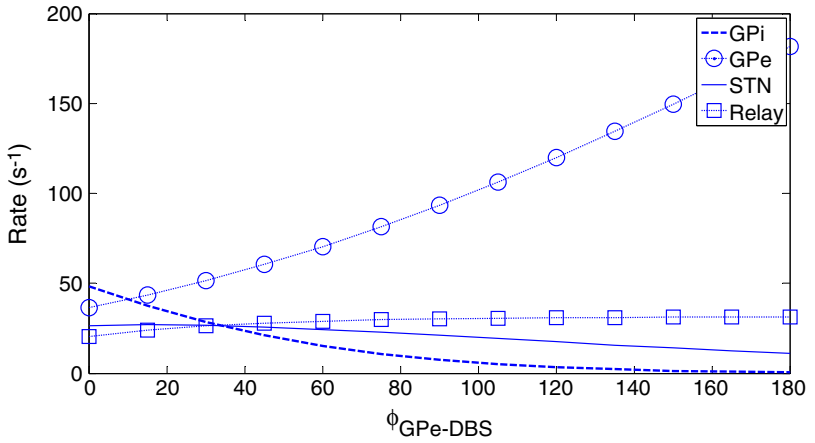

Fig. 3. Mean firing rates of GPi, GPe, STN, and thalamic relay nucleus during GPe-DBS. Dashed, GPi; circle-dotted, GPe; solid, STN; square-dotted, thalamic relay nucleus.

For DBS above 120 Hz, the rate of GPe still increase with the DBS stimuli. The rate of STN still decreases with the DBS stimuli. The total inhibition from GPe conquest the total excitation input from STN and GPi cells were completely inhibited by the inhibitory input from GPe. The rate of thalamic relay nucleus still has fixed values during increase in DBS frequency.

3.3. *GPi-DBS*

Here DBS was applied to GPi. Changes in firing rates due to GPi-DBS, are shown in Fig. 4.

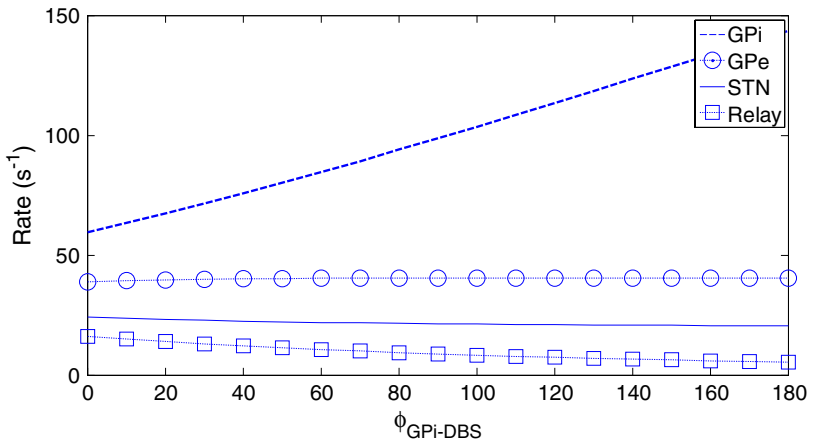

Fig. 4. Mean firing rates of GPi, GPe, STN, and thalamic relay nucleus during GPi-DBS. Dashed, GPi; circle-dotted, GPe; solid, STN; square-dotted, thalamic relay nucleus.

The rate of pathologic GPe was not changed by GPi-DBS and the rate of STN was decreased by GPi-DBS slightly.

The rate of GPi increases monotonically due to increase in DBS frequency.

The rate of thalamic relay nucleus increases monotonically due to monotonically increasing inhibitory input from GPi.

4. Discussion

4.1. *Effects of stimulation site and DBS frequency*

Simulation results (Figs. 2–4) indicated that:

- GPi-DBS modulated the rate of GPi at levels that could lead to an inhibition (GPi-DBS) of the thalamic relay nucleus. This effect increased monotonically with the DBS frequency.
  The effects of STN- and GPe-DBS on the rate of GPi and the thalamic relay nucleus are not so easy to interpret, due to the direct (STN $\xrightarrow{+}$ GPi, GPe $\xrightarrow{-}$ GPi) and indirect (STN $\xrightarrow{+}$ GPe $\xrightarrow{-}$ GPi, GPe $\xrightarrow{-}$ STN $\xrightarrow{+}$ GPi) pathways from STN and GPe to GPi.
- STN-DBS allowed the overall recovery of the thalamic relay nucleus responsiveness for every tested DBS frequency. However, the recovery was heavily influenced by the DBS frequency, as can be inferred by the rate of GPi. During DBS up to 120 Hz, the rate of STN increases with DBS stimuli. GPe, excited by STN, increase with DBS. The resulting contributions to GPi lead to a decrease in its rate. During DBS above 120 Hz, the rates of STN and GPe cells still increase with the DBS stimuli, leading (a) the total inhibition from GPe activity to progressively override the total excitation from the STN activity and (b) GPi to be completely inhibited by the GPe activity above 120 Hz and (c) rate of thalamic relay nucleus activated by deactivation of GPi.
- GPe-DBS allowed the overall recovery of the thalamic relay nucleus responsiveness for every tested DBS frequency. During DBS up to 40 Hz, the rate of GPe increases with DBS stimuli. STN increases slightly with DBS. The resulting contributions to GPi lead to a decrease in its rate. During DBS above 40 Hz, GPe still increase with the DBS stimuli, but STN inhibited by high rate of GPe as DBS frequency increases. This lead to attenuation of excitatory input from STN to GPi, leading (a) the inhibition from GPe activity to progressively override the total attenuated excitation from the STN activity and (b) GPi to be completely inhibited by the GPe activity above 120 Hz and (c) rate of thalamic relay nucleus activated by deactivation of GPi.

Thus, GPi-DBS led to an inhibition of the thalamic relay nucleus activity. The control mechanism was potentially restored during STN- and GPe-DBS.

4.2. *Thalamic activity in normal and PD states and during DBS*

Thalamic activity and the inhibitory input from GPi to thalamus are illustrated in Figs. 2–4.

In the normal state, the inhibitory input of the GPi to the thalamus does not decrease the thalamic relay nucleus activity.

In the PD state, the inhibitory input of GPi to the thalamus leads to a decrease of thalamic relay nucleus activity. The rate of this inhibition is high enough to inhibit thalamic relay nucleus activity.

STN-DBS and GPe-DBS stabilize the inhibitory input from GPi to thalamus at a low level. Therefore increase of thalamic relay nucleus activity is obtained by STN-DBS and GPe-DBS.

GPi-DBS stabilizes the input from GPi to thalamus contribution at a high level. Therefore a decrease in thalamic relay nucleus activity is obtained by applying DBS of GPi.

4.3. *DBS sites: experimental evidence versus simulation results*

The frequency used for the DBS plays an important role in PD treatment. Low-frequency GPi-DBS was not sufficient to drive an increase in the thalamic relay nucleus activity toward an inhibition (GPi-DBS). Low-frequency STN- and GPe-DBS was instead sufficient to drive a restoration of the control mechanism, but, interestingly, only high-frequency STN- and GPe-DBS (above 120 Hz) was able to restore the control mechanism completely.

Our findings agree with experimental evidences about the DBS effects achieved in human subjects and monkeys by micro-dialysis and extracellular recording procedures. Micro-dialysis evidences in PD subjects suggest that STN-DBS increases the STN activity,[15] and augments STN-driven excitation of GPi, while simultaneously decreasing GABA extracellular concentrations in the anteroventral thalamus, one of the thalamic relay nuclei targeted by GPi.[16] These speculations are confirmed by our simulation results, which suggest a simultaneous activation of STN and inhibition of GPi during STN-DBS. Indeed, rate of GPi was lower in the STN-DBS state than in the normal or PD ones.

Our findings are also consistent with results obtained by Kita and colleagues,[17] on monkeys. In their work, single pulses and high-frequency stimulations (110 Hz) of STN evoked powerful excitatory responses in GPe neurons, while evoking a predominantly inhibitory response in GPi neurons. Their data suggest that the STN $\overset{+}{\rightarrow}$ GPe excitatory response dominates the STN $\overset{+}{\rightarrow}$ GPe $\overset{-}{\rightarrow}$ GPe recurrent inhibition in the GPe, whereas the STN $\overset{+}{\rightarrow}$ GPe $\overset{-}{\rightarrow}$ GPi inhibitory response dominates the STN $\overset{+}{\rightarrow}$ GPi excitatory response in the GPi.

Simulation results showed that GPi-DBS acted to: (a) stabilize the GPi $\rightarrow$ thalamus inhibition at a level that is as high as the DBS frequency and (b) progressively inhibit thalamic relay nucleus as DBS frequency increases. These results are consistent with those from Ref. 18 in an extracellular recording study in monkeys, where high-frequency stimulation of GPi at (100 Hz) inhibited or decreased the activity of most of the thalamic cells.

4.4. *Simulation results and clinical evidence*

In clinical practice, the preferred surgical target for DBS in the treatment of PD is the STN. However, results from randomized studies recently showed that each of these three nuclei, STN, GPe, and GPi are effective DBS targets, leading to a renewed interest in GPi and GPe as DBS targets for PD and to the formation of other randomized studies.[19]

As stated before, our simulations approach: outlines two different effects that could be associated with STN-, GPe-, and GPi-DBS. Consequently, within this model we could relate bradykinetic and akinetic aspects of PD to the weak rate of thalamic relay nucleus due to PD state.

We will read here our results from simulations using BGTCS model in the light of the few elements that the clinical literature provides as distinctive of STN, GPe, and GPi targets or as part of the common expert clinical judgments in the decision about the preferred surgical target for a specific PD patient.

The inhibition of thalamic relay nucleus activity that we observed as a result of the high-frequency GPi-DBS could be responsible for the larger control of dyskinesia observed by skilled surgeons in GPi-DBS. Our results could suggest that GPi is an ideal target for patients mostly impaired by hyperkinetic signs of PD.

Bradykinesia tends to be improved more with STN-DBS than with GPi-DBS.[20] This observation is consistent with the increase in rate of thalamic relay nucleus due to STN-DBS.

Finally, it has been observed that GPe-DBS improves bradykinesia and akinesia compared to GPi-DBS, and GPe-DBS induces more dyskinetic events than GPi-DBS.[21–24] This observation is consistent with increase in the rate of thalamic relay nucleus due to GPe-DBS.

Consequently based on our results, we conclude that stimulation of STN or GPe speeds up the execution of movements and that STN and GPe could be ideal targets for patients mostly impaired by hypokinetic signs of PD.

5. Conclusion

In the present study, we used a computational model of the BGTCS, to compare the different effects of DBS of STN, GPe, and GPi for PD. To this end, a mean-field model of the BGTCS is used. This model was able to reproduce both the physiological and pathological activities of BG, thalamus and motor cortex in a unified structure. Using a mean-field model of the BGTCS allowing a more complete framework to simulate DBS and to interpret its effects in the BGTCS. Also, this model is more reliable than earlier models because it has complete circuitry of the basal ganglia (all nuclei and their interactions). Moreover, it considers the thalamus and the motor cortex which were rarely considered in the earlier models. Finally, we believe BGTCS is better than earlier models since it is more controllable for larger network models of the BGTCS than those which have been used so far for DBS.

Consequently, our findings suggest that DBS in the STN and GPe could restore the thalamus relay activity, while DBS in the GPi could inhibit it. Also our results

were consistent with experimental evidences regarding STN-and GPi-DBS and several comparative clinical evidences regarding STN-, GPe-, and GPi-DBS.

References

1. Bar-Gad I, Morris G, Bergman H, Information processing, dimensionality reduction and reinforcement learning in the basal ganglia, *Prog Neurobiol* **71**:439−473, 2003.
2. Paxinos G, Mai J, The basal ganglia, *The Human Nervous System*, Elsevier, Amsterdam, pp. 676−738, 2004.
3. Walters JR, Hu D, Itoga CA, Parr-Brownlie LC, Bergstrom DA, Phase relationships support a role for coordinated activity in the indirect pathway in organizing slow oscillations in basal ganglia output after loss of dopamine, *Neuroscience* **144**:762−776, 2007.
4. Parkinson J, *An Essay on the Shaking Palsy*, Sherwood, Neely, and Jones, London, 1817.
5. Bergman H, Deuschl G, Pathophysiology of Parkinson's disease: From clinical neurology to basic neuroscience and back, *Mov Disord* **17**:28−40, 2002.
6. Bergman H, Wichmann T, Karmon B, DeLong MR, The primate subthalamic nucleus. II. Neuronal activity in the MPTP model of parkinsonism, *J Neurophys* **72**:507−520, 1994.
7. Chang JY, Shi LH, Luo F, Zhang WM, Woodward DJ, Studies of the neural mechanisms of deep brain stimulation in rodent models of Parkinson's disease, *Neurosci Biobehav Rev* **32**:352−366, 2008.
8. Limousin P, Krack P, Pollak P, Benazzouz A, Ardouin C, Hoffmann D, Benabid A-L, Electrical stimulation of the subthalamic nucleus in advanced Parkinson's disease, *N Engl J Med* **339**:1105−1111, 1998.
9. Meissner W, Leblois A, Hansel D, Bioulac B, Gross C, Benazzouz A, Boraud T, Subthalamic high frequency stimulation resets subthalamic firing and reduces abnormal oscillations, *Brain* **128**:2372−2382, 2005.
10. Johnson MD, Miocinovic S, McIntyre CC, Vitek JL, Mechanisms and targets of deep brain stimulation in movement disorders, *Neurotherapeutics* **5**:294−308, 2008.
11. Rubin JE, Terman D, High frequency stimulation of the subthalamic nucleus eliminates pathological thalamic rhythmicity in a computational model, *J Comput Neurosci* **16**:211−235, 2004.
12. Modolo J, Mosekilde E, Beuter A, New insights offered by a computational model of deep brain stimulation, *J Physiol Paris* **101**:56−63, 2007.
13. Van Albada SJ, Robinson PA, Mean-field modeling of the basal ganglia-thalamocortical system. I. Firing rates in healthy and parkinsonian states, *J Theor Biol* **257**:642−663, 2009.
14. Nahvi A, Bahrami F, Which one is more effective in Parkinson's Disease? Stimulating the motor cortex or the basal ganglia?, *17th Iranian Conference of Biomedical Engineering* (*ICBME2010*), Isfahan, Iran, November 3−4, 2010, Doi: 10.1109/ICBME.2010.5704973.
15. Stefani A, Fedele E, Galati S, Pepicelli O, Frasca S, Pierantozzi M *et al.*, Subthalamic stimulation activates internal pallidus: Evidence from cGMP microdialysis in PD patients, *Ann Neurol* **57**:448−452, 2005.
16. Stefani A, Fedele E, Galati S, Raiteri M, Pepicelli O, Brusa L *et al.*, Deep brain stimulation in Parkinson's disease patients: Biochemical evidence, *J Neural Transm Suppl* **70**:401−408, 2006.
17. Kita H, Tachibana Y, Nambu A, Chiken S, Balance of monosynaptic excitatory and disynaptic inhibitory responses of the globus pallidus induced after stimulation of the subthalamic nucleus in the monkey, *J Neurosci* **25**:8611−8619, 2005.
18. Anderson ME, Postupna N, Ruffo M, Effects of high-frequency stimulation in the internal globus pallidus on the activity of thalamic neurons in the awake monkey, *J Neurophys* **89**:1150−1160, 2003.

19. Weaver F, Follett K, Hur K, Ippolito D, Stern M, Deep brain stimulation in Parkinson disease: A metaanalysis of patient outcomes, *J Neurosurg* **103**:956−967, 2005.
20. Ostergaard K, Sunde NA, Evolution of Parkinson's disease during 4 years of bilateral deep brain stimulation of the subthalamic nucleus, *Mov Disord* **21**:624−631, 2006.
21. Payoux P, Remy P, Miloudi M, Houeto JL, Stadler C, Bejjani BP *et al.*, Contrasting changes in cortical activation induced by acute high-frequency stimulation within the globus pallidus in Parkinson's disease, *J Cereb Blood Flow Metabol* **29**:235−243, 2009.
22. Vitek JL, Hashimoto T, Peoples J, DeLong MR, Bakay RAE, Acute stimulation in the external segment of the globus pallidus improves Parkinsonian motor signs, *Mov Disord* **19**:907−915, 2004.
23. Yelnik J, Damier P, Bejjani BP, Francois C, Gervais D, Dormont D *et al.*, Functional mapping of the human globus pallidus: Contrasting effect of stimulation in the internal and external pallidum in Parkinson's disease, *J Neurosci* **101**:77−87, 2000.
24. Krack P, Pollak P, Limousin P, Hoffmann D, Benazzouz A, Le Bas JF *et al.*, Opposite Motor Effects of Pallidal Stimulation in Parkinson's Disease," *Ann Neurol* **43**:180−192, 1998.

Appendix

The relevant parameters for healthy subjects are presented in Table 1. See Ref. 13 for more details on parameters used.

Table 1. The parameters for healthy state used in the BGTCS (see Ref. 13).

Quantity	Symbol	Value	Unit	Quantity	Symbol	Value	Unit
Maximum firing rate				Maximum firing rate			
Cortex	$Q_e^{\max}$, $Q_i^{\max}$	300	s^{-1}	STN	$Q_s^{\max}$	500	s^{-1}
Striatum	$Q_{d1}^{\max}$, $Q_{d2}^{\max}$	65	s^{-1}	Relay nuclei	$Q_t^{\max}$	300	s^{-1}
GPi	$Q_{p1}^{\max}$	250	s^{-1}	TRN	$Q_r^{\max}$	500	s^{-1}
GPe	$Q_{p2}^{\max}$	300	s^{-1}				
Firing threshold				Firing threshold			
Cortex	θ_e, θ_i	14	mV	STN	θ_s	12	mV
Striatum	θ_{d1}, θ_{d2}	19	mV	Relay nuclei	θ_t	13	mV
GPi/SNr	θ_{p1}	8	mV	TRN	θ_r	13	mV
GPe	θ_{p2}	12	mV				
Threshold spread	σ'	3.8	mV				
Connection strength				Connection strength			
ee, *ie*	ν_{ee}, ν_{ie}	1.6	mV s	*p*2*d*2	ν_{p2d2}	−0.3	mV s
ei, *ii*	ν_{ei}, ν_{ii}	−1.9	mV s	*p*2*p*2	ν_{p2p2}	−0.1	mV s
et, *it*	ν_{et}, ν_{it}	0.4	mV s	*p*2*s*	ν_{p2s}	0.5	mV s
*d*1*e*	ν_{d1e}	1.0	mV s	*se*	ν_{se}	0.1	mV s
*d*1*d*1	ν_{d1d1}	−0.3	mV s	*sp*2	ν_{sp2}	−0.03	mV s
*d*1*t*	ν_{d1t}	0.1	mV s	*te*	ν_{te}	0.8	mV s
*d*2*e*	ν_{d2e}	0.7	mV s	*tp*1	ν_{tp1}	−0.03	mV s

Table 1. (*Continued*)

Quantity	Symbol	Value	Unit	Quantity	Symbol	Value	Unit
$d2d2$	ν_{d2d2}	-0.3	mV s	tr	ν_{tr}	-0.4	mV s
$d2t$	ν_{d2t}	0.05	mV s	tn	ν_{tn}	0.5	mV s
$p1d1$	ν_{p1d1}	-0.1	mV s	re	ν_{re}	0.15	mV s
$p1p2$	ν_{p1p2}	-0.03	mV s	rt	ν_{rt}	0.03	mV s
$p1s$	ν_{p1s}	0.1	mV s				